AL-1984

ORNL-TM-5113

Comparison of Hansen-Roach and ENDF/B-IV Cross Sections for ^{233}U Criticality Calculations

S. R. McNeany
J. D. Jenkins

OAK RIDGE NATIONAL LABORATORY
OPERATED BY UNION CARBIDE CORPORATION • FOR THE U.S. ATOMIC ENERGY COMMISSION

BLANK PAGE

Printed in the United States of America. Available from
National Technical Information Service
U.S. Department of Commerce
5285 Port Royal Road, Springfield, Virginia 22161
Price: Printed Copy $5.00; Microfiche $2.25

ORNL-TM-5113

UC-77 — Gas-Cooled Reactor Technology

Contract No. W-7405-eng-26

Reactor Division

COMPARISON OF HANSEN-ROACH AND ENDF/B-IV CROSS SECTIONS FOR ^{233}U CRITICALITY CALCULATIONS

S. R. McNeany J. D. Jenkins

JANUARY 1976

NOTICE: This document contains information of a preliminary nature and was prepared primarily for internal use at the Oak Ridge National Laboratory. It is subject to revision or correction and therefore does not represent a final report.

OAK RIDGE NATIONAL LABORATORY
Oak Ridge, Tennessee 37830
operated by
UNION CARBIDE CORPORATION
for the
U.S. ENERGY RESEARCH AND DEVELOPMENT ADMINISTRATION

CONTENTS

COMPARISON OF HANSEN-ROACH AND ENDF/B-IV CROSS SECTIONS FOR ^{233}U CRITICALITY CALCULATIONS

S. R. McNeany J. D. Jenkins

ABSTRACT

A comparison is made between criticality calculations performed using ENDF/B-IV cross sections and the 16-group Hansen-Roach library at ORNL. The area investigated is homogeneous systems of highly enriched ^{233}U in simple geometries. Calculations are compared with experimental data for a wide range of $H/^{233}U$ ratios. Results show that calculations of k_{eff} made with the Hansen-Roach cross sections agree within 1.5% for the experiments considered. Results using ENDF/B-IV cross sections were in good agreement for well-thermalized systems, but discrepancies up to 7% in k_{eff} were observed in fast and epithermal systems.

Key words: Hansen-Roach, ENDF/B-IV, cross sections, criticality, ^{233}U, reactivity calculations.

INTRODUCTION

The Metals and Ceramics Division of Oak Ridge National Laboratory (ORNL) is presently designing a nuclear fuel refabrication facility to produce recycle fuel elements for the High-Temperature Gas-Cooled Reactor (HTGR). Highly enriched ^{233}U comprises the fissile material in these elements. Part of the design effort is the determination of equipment size limitations due to criticality considerations. Up to the present time, all criticality calculations required for the plant have utilized the 16-group Hansen-Roach (H-R) cross section set[1] at ORNL. Recently, some ^{233}U criticality calculations were performed at Battelle Pacific Northwest Laboratories (BPNL) using ENDF/B-III cross sections.[2] These were compared with a calculational survey made at Oak Ridge in 1973 using H-R cross sections.[3] The agreement was poor. In fact, in one case where the system contained ^{232}Th in addition to ^{233}U, there was a difference of nearly 50% in critical mass. No experimental data are available on these calculated systems; hence neither analysis could be directly confirmed.

The purpose of this study was to analyze the H-R and ENDF/B-IV cross-section sets through comparison with some limited experimental data and further comparison with the earlier calculational survey. The ORNL processing codes were used for the calculations.

The main text of this report is divided into three parts. The first section presents the calculational techniques used, along with a brief description of the cross section sets. Next, the results of calculations made with H-R and ENDF/B-IV cross sections are compared with the experimental results. The third section presents the results of the Battelle calculations and those of the present work in comparison with the above calculational survey. An appendix is included which supplies information on the geometry and atomic composition of all the systems calculated in this work.

CALCULATIONAL TECHNIQUE

Cross-Section Sets

Two cross-section sets were used in this study. The first is the ENDF/B-IV library which is available from Brookhaven National Laboratory (BNL), and the second is a 16-group Hansen-Roach library used at ORNL. Both of these libraries have been described in the literature;[1,2] consequently, only the processing of the data is described here.

To utilize the ENDF data for criticality calculations, a 123-energy-group P_3 "master library" was generated. This library consists of flux-averaged smooth cross sections plus resonance parameters. The assumed flux shape used in the fine-group averaging procedure was a Maxwellian (at 300°K) from zero to 0.1265 eV connected to a 1/E spectrum which continued up to 67.4 keV, where it was connected to a Maxwellian fission spectrum with an effective temperature of 1.273 MeV. XLACS, a processing code which is part of the AMPX code package,[4] was used to generate the master library. NITAWL, also part of the AMPX package, forms problem-dependent, resonance self-shielded cross sections from the master library for later use in criticality calculations.

The second cross-section set used in this investigation is the 16-group Hansen-Roach set. Some of the nuclides in this library contain a P_0 and a P_1 set, while others have only a P_0 set. No resonance parameters are given. Resonance self-shielding is accounted for by the inclusion of multiple cross-section sets for resonance nuclides (i.e., those nuclides where resonance self-shielding may play an important role). The selection of a particular set for a resonance nuclide is made on the basis of a problem-dependent, potential scattering cross section per atom of resonance nuclide (σ_p) in the medium containing the resonance nuclide:

$$\sigma_p = \frac{\sum_{i \neq res} N_i \sigma_{si}}{N_{res}} ,$$

where

N_i = number density of the ith nuclide in the mixture,

σ_{si} = potential scattering cross section of the ith nuclide in the mixture,

N_{res} = number density of the resonance nuclide,

$\sum_{i \neq res} N_i \sigma_{si}$ = macroscopic potential scattering cross section for the mixture excluding the resonance nuclide.

Processing Codes

The following is a list of the ORNL computer codes used in this work along with a short description of each.

(1) ANISN — ANISN solves the one-dimensional Boltzmann transport equation for a slab, cylinder, or sphere by the discrete ordinates (S_N) method.[5] It also has the capability to perform a group reduction of cross sections through the use of the flux generated as the solution of the Boltzmann equation.

(2) AMPX — AMPX is a modular code system[4] for generating coupled multigroup neutron-gamma libraries from ENDF/B. It embodies codes (2a) through (2e) as some of its modules.

(2a) XLACS — This module produces flux-weighted multigroup neutron cross sections from ENDF/B. It treats the full energy range and can expand anisotropic processes to any order Legendre polynomial.

(2b) RADE — This module performs checks on the multigroup libraries produced by AMPX modules. Checks include: (i) Does the sum of partial cross sections equal the corresponding total cross section? (ii) Are all the one-dimensional and P_0 two-dimensional cross sections non-negative? and (iii) Is $|\bar{\mu}| \leq 1$ for all group-to-group transfer cross sections?

(2c) NITAWL — This module produces a resonance self-shielded working library suitable for use in a transport calculation. NITAWL uses the Nordheim integral treatment[6] to account for problem-dependent resonance self-shielding effects.

(2d) XSDRNPM — This is a one-dimensional transport theory code capable of calculating reaction rates, effective multiplication factors (k_{eff}), and critical dimensions. It contains the features of ANISN and handles the cross-section format generated by NITAWL for a working library.

(2e) KENO — This is a three-dimensional Monte Carlo code especially useful for making criticality calculations. Like XSDRNPM and ANISN, it calculates reaction rates, effective multiplication factors, and critical dimensions. It also calculates the standard deviation on its result, an inherent characteristic of Monte Carlo codes.

Processing Procedure

The starting point of our criticality calculations is formed by our two basic cross-section libraries — the 123-group ENDF-based master library and the 16-group H-R library. To perform a criticality calculation using ENDF/B data, it is first necessary to produce a problem-dependent working library with NITAWL. This library is then used by XSDRNPM or

KENO, depending on the problem geometry, to calculate the effect of interest (i.e., k_{eff}, critical radius, etc.).

Hansen-Roach calculations require the determination of σ_p for each resonance nuclide in the problem. These σ_p's then form the basis for selection of resonance nuclide cross-section sets to be used by ANISN or KENO to calculate the effect of interest.

RESULTS OF CALCULATIONS ON CRITICAL EXPERIMENTS

^{233}U Critical Experiments

An important parameter in criticality calculations is the hydrogen-to-uranium number density ratio (H/U) of the particular problem being studied. This parameter has a controlling effect on the shape of the neutron energy spectrum and hence gives an indication of which energy regions (and cross-section groups) contribute most to the effect of interest. The larger the H/U ratio, the more thermalized is the neutron flux. For example, in a ^{233}U metal sphere with a $H/^{233}U$ ratio of zero, the high-energy groups are the main contributors to a k_{eff} determination. Less than 10^{-8}% of the total number of fissions take place in the energy range below 1.86 eV, which indicates that the thermal cross sections are not important in this problem. On the other hand, a problem having a $H/^{233}U$ ratio of 1533 has more than 96% of the fissions taking place in the thermal energy range. Here, the thermal cross sections are very important.

Six highly enriched ^{233}U critical experiments having $H/^{233}U$ ratios of 0, 39.4,* 154, 381, 1533, and 1986 were selected from the literature. Using the given descriptions of material compositions and geometries, k_{eff} was calculated for each experiment with both cross-section libraries. The results of these calculations are given in Table 1 and Fig. 1. The errors indicated in the table and the error bars shown on the figure represent one standard deviation as calculated by the Monte Carlo code KENO. To check agreement between KENO and XSDRNPM (a discrete-ordinates code), two

*This experiment was fully reflected by paraffin; consequently, it has an effective $H/^{233}U$ ratio which is higher than the stated value for the core.

Table 1. Results of Hansen-Roach and ENDF/B cross-section calculations on some highly enriched ^{233}U critical experiments

Experiment No.	Critical experiment (highly enriched with ^{233}U)	$H/^{233}U$ ratio	Calculated k_{eff}[a]	
			Hansen-Roach	ENDF/B-IV
1	Unreflected sphere of U metal[7]	0.0	1.007 (ANISN)[b]	0.966 (XSDRNPM)
2	Fully reflected finite cylinder of aqueous UO_2F_2 solution[8]	39.4	1.006±0.007 (KENO)	1.069±0.006 (KENO)
3	Unreflected finite cylinder of aqueous UO_2F_2 solution[8]	154	0.990±0.006 (KENO)	1 027±0.007 (KENO)
4	Unreflected sphere of aqueous UO_2F_2 solution[8]	381	0.988 (ANISN)	1.034 (XSDRNPM) 1.026±0.006 (KENO)
5	Unreflected sphere of aqueous $UO_2(NO_3)_2$ solution[7]	1533	1.004 (ANISN)	1.003 (XSDRNPM) 1.005±0.003 (KENO)
6	Unreflected sphere of aqueous $UO_2(NO_3)_2$ solution[9]	1986	1.005 (ANISN)	0.994 (XSDRNPM)

[a] Errors represent one standard deviation on calculated mean value.

[b] Names in parentheses indicate codes used to calculate k_{eff}.

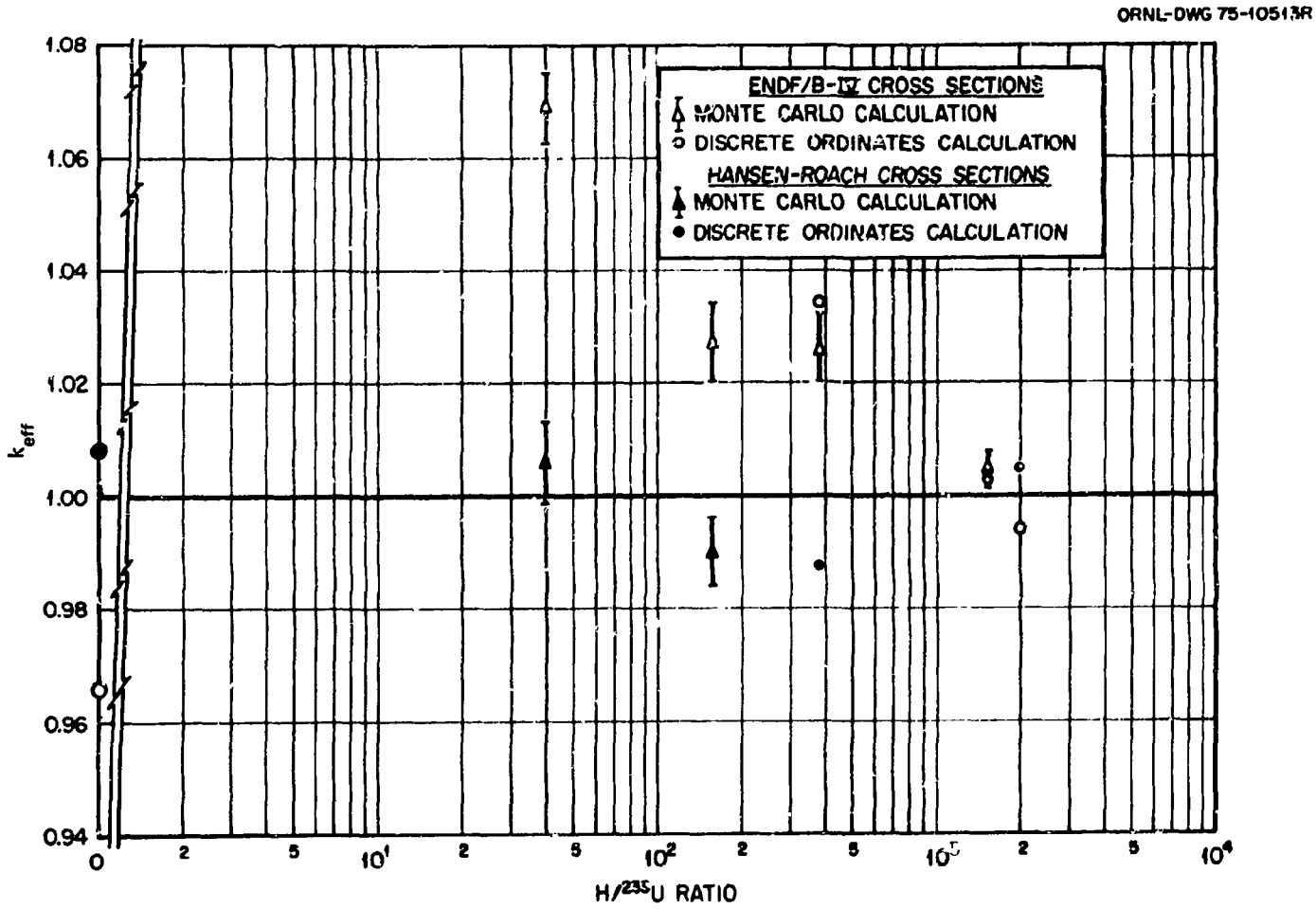

Fig. 1. Comparison between ENDF/B-IV and Hansen-Roach cross sections for ^{233}U criticality calculations.

of the experiments were calculated by both codes. In both cases, the KENO result fell within two standard deviations (95% confidence interval) of the XSDRNPM result. Hence, the agreement between the codes was as good as can be expected in view of the statistical process of a Monte Carlo calculation.

As a point of clarification, the cylindrical geometry experiments were calculated only with the Monte Carlo code because a 123-group two-dimensional discrete-ordinates calculation would have been much more costly in terms of computer time.

The results of the calculations show good agreement between the H-R calculations and the six experiments. For well-thermalized systems (i.e., $H/^{233}U$ ratios of 1500–2000), ENDF/B cross sections agree well with the experiments. However, as the $H/^{233}U$ ratio is decreased from the well-thermalized systems, significant deviations are observed between ENDF/B calculations and the experiments.

As stated above, the energy dependence of the fission rate is an indicator of which energy regions are important in determining k_{eff}. Consequently, the energy-dependent fission rate was calculated for each of the ^{233}U critical experiments. Figure 2 shows a plot of the calculated fission rate per unit lethargy as a function of energy for three of the experiments. Experiment 1, a ^{233}U metal sphere, displays a characteristic fast spectrum, while experiment 5, having an $H/^{233}U$ ratio of 1533, exhibits a well-thermalized system. Experiment 2, with a core $H/^{233}U$ ratio of 39.4, has some epithermal character. To put these statements on a quantitative basis, consider the full energy range to be composed of three regions — a thermal region from 0 to 1.86 eV, an epithermal region from 1.86 eV to 111 keV, and a fast region from 111 keV to 14.92 MeV. Table 2 lists the percentage of fissions occurring in each region for the six ^{233}U experiments under consideration. The table shows how the fission rate energy spectrum increases in epithermal character and finally fast character as the $H/^{233}U$ ratio is decreased from the well-thermalized systems.

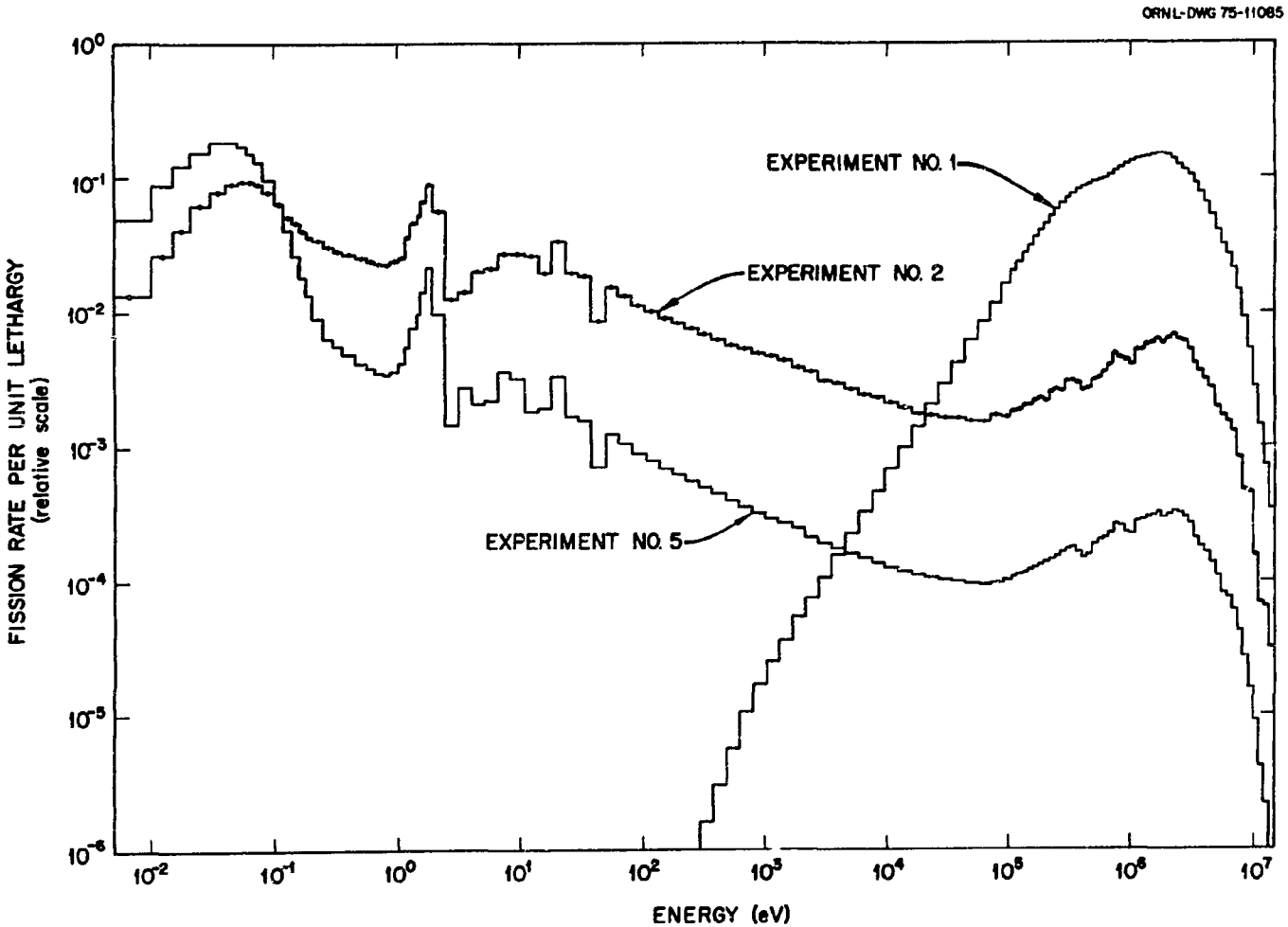

Fig. 2. Energy-dependent fission rate for three ^{233}U critical experiments.

Table 2. Calculated energy dependence of fissions in six ^{233}U critical experiments

Experiment No.	$H/^{233}U$ ratio	Percent of fissions		
		Thermal (0–1.86 eV)	Epithermal (1.86 eV–111 keV)	Fast (111 keV–14.92 MeV)
1	0.0	$<10^{-8}$	3.84	96.16
2	39.4	67.19	28.96	3.85
3	154	82.90	15.55	1.55
4	381	91.58	7.79	0.631
5	1533	96.82	2.98	0.203
6	1986	97.28	2.55	0.169

^{235}U Critical Experiments

As a check on the processing codes and the cross-section sets, calculations were made on two highly enriched ^{235}U critical experiments. An unreflected ^{235}U metal sphere was selected along with an unreflected sphere of aqueous UO_2F_2 solution having a $H/^{235}U$ ratio of 1393. The results are given in Table 3. As seen in the table, the agreement between the calculations and the experiments is good. This result tends to justify the validity of the processing procedure for ENDF/B data for isotopes other than ^{233}U.

Table 3. Results of Hansen-Roach and ENDF/B cross-section calculations on two highly enriched ^{235}U experiments

Experiment No.	Critical experiment (highly enriched with ^{235}U)	$H/^{233}U$ ratio	Calculated k_{eff}[a]	
			Hansen-Roach	ENDF/B-IV
7	Unreflected sphere of uranium metal[10]	0.0	1.001 (ANISN)[b]	1.008 (XSDRNPM)
8	Unreflected sphere of aqueous UO_2F_2 solution[11]	1393	1.009 (ANISN)	1.006±0.004 (KENO)

[a] Errors represent one standard deviation.
[b] Names in parentheses indicate codes used to calculate k_{eff}.

RESULTS OF CALCULATIONS ON THEORETICAL ^{233}U SYSTEMS

In April 1973, a report[3] was issued at Oak Ridge on ^{233}U criticality calculations performed in support of the HTGR fuel refabrication process. These are simple geometry calculations to be used as guidelines in criticality control. The 16-group Hansen-Roach cross section set at ORNL was used in the calculations. In June 1975, a report[12] was issued by BPNL in which several of the calculations from the above Oak Ridge report were reproduced using ENDF/B-III cross sections. The BPNL report indicated large differences in computed critical masses between the ENDF and H-R results. In particular, differences ranged between 14% and 56% for cases of water-reflected homogeneous spheres of ^{233}U and ^{233}U-^{232}Th mixtures. Table 4, which is taken directly from the BPNL report, gives the results of their calculations in comparison with the 1973 Oak Ridge report.

As a further investigation of the differences in the calculated results, the top three cases in Table 4 were calculated using our 123-energy-group master library and the H-R library. As expected, the results of the H-R calculations were identical to those of the earlier Oak Ridge report. For the ENDF comparison, k_{eff} was calculated for each case using the BPNL results for the critical radius. Table 5 presents the results of these calculations. Based on the results of Table 5, we believe that the discrepancies observed by BPNL have been confirmed by our calculations.

CONCLUSIONS

As a result of the studies made during the course of this work, we have reached the following conclusions.

1. The 16-energy-group Hansen-Roach cross-section set presently used at ORNL is adequate for criticality safety calculations on homogeneous pure ^{233}U systems (i.e., systems containing ^{233}U as the prime heavy-metal constituent) with $H/^{233}U$ ratios of ~40 to 2000 and metal systems.
2. To the authors' knowledge, no experimental criticality data are available on highly enriched ^{233}U systems having $H/^{233}U$ ratios of 10 to 30.*

*$H/^{233}U$ ratios of 10 to 30 are characteristic of some fuel forms which may be present in an HTGR fuel refabrication facility.

Table 4. Comparison between calculated critical conditions for homogeneous fuel mixtures typical of the HTGR fuel cycle[12]

$H/^{233}U$ (atom ratio)	$C/^{233}U$ (atom ratio)	^{233}U (g/cm^3)	Water-reflected spheres			
			ENDF/B + DTF-IV[a]		H-R + ANISN[b]	
			Critical radius (cm)	Critical mass (kg ^{233}U)	Critical radius (cm)	Critical mass (kg ^{233}U)
			0 $^{232}Th/^{233}U$			
2	0	5.433	7.64	10.15	8.25	12.77
2	100	0.328	26.17	24.62	29.5	35.27
500	100	0.045	14.44	0.56	15.1	0.65
			4 $^{232}Th/^{233}U$			
2	0	1.568[c]	17.02	32.38	18.95	46.61
2	122.1	0.242[c]	36.82	50.60	42.55	78.73
500	122.1	0.043	16.02	0.74	16.81	0.85

[a]Calculated values using ENDF/B data processed by ETOG and FLANGE and averaged over 18 energy groups by EGGNIT for use in DTF-IV.
[b]Calculated values reported by Thomas.[3]
[c]Higher densities reported in Ref. 3 as a result of using an oxide density of 10.65 g/cm^3 instead of a mixture density based on 10.65 g UO_2/cm^3 and 10.03 g ThO_2/cm^3.

Table 5. ENDF/B-IV calculations of k_{eff} for three ^{233}U systems

Case No.	$H/^{233}U$ ratio	$C/^{233}U$ ratio	^{233}U (g/cm^3)	Critical radius[a] (cm)	k_{eff}[b]
1	2	0	5.433	7.64	0.979±0.009 (KENO)
2	2	100	0.328	26.17	1.000 (XSDRNPM)
3	500	100	0.045	14.44	0.996 (XSDRNPM)

[a]BPNL calculation.
[b]Present work.

Hence, no cross-section set was directly confirmed for these systems. Interpolation of results between higher H/^{233}U ratios and zero may not be valid because the neutron energy spectrum changes drastically between these bounds.

3. Calculational discrepancies between ENDF/B and Hansen-Roach cross sections for highly enriched ^{233}U systems have been confirmed by this work. In particular, a comparison of ENDF/B calculational results with experimental data for highly enriched ^{233}U systems indicates significant problems with ENDF/B results on systems having H/^{233}U ratios less than 400.

ACKNOWLEDGMENTS

The authors wish to express their appreciation to the others who contributed to this work. Special thanks are due to N. M. Greene of the Computer Sciences Division for his assistance and advice on running the computer codes. The artistic contributions of A. G. Mason and H. R. Livesey in the preparation of the figures are appreciated. In addition, thanks are due to J. Renfro and R. L. Castleberry for typing the draft copies; J. T. Thomas and N. M. Greene for their critical reviews; A. Ragan and M. R. Sheldon for their editorial assistance and M. H. Wilson for typing the final copy.

REFERENCES

1. G. E. Hansen and W. H. Roach, *Six and Sixteen Group Cross Sections for Fast and Intermediate Critical Assemblies*, LAMS-2543, Los Alamos Scientific Laboratory (1961).

2. M. K. Drake (Ed.), *Data Formats and Procedures for the ENDF Neutron Cross Section Library*, BNL-50274 (T-601), Brookhaven National Laboratory (October 1970).

3. J. T. Thomas, *Calculated Criticality of Water Moderated Oxides of Uranium-233, Thorium-232, and Carbon Mixtures*, Y-DR-107, Union Carbide Corporation, Y-12 Plant (1973).

4. N. M. Greene et al., *AMPX: A Modular Code System for Generating Coupled Multigroup Neutron-Gamma Libraries from ENDF/B*, ORNL-TM-3706 (draft).

5. W. W. Engle, Jr., *A Users Manual for ANISN: A One-Dimensional Discrete Ordinates Transport Code with Anisotropic Scattering*, K-1693, Union Carbide Corporation Nuclear Division, Oak Ridge Gaseous Diffusion Plant (1967).

6. L. W. Nordheim, "The Theory of Resonance Absorption," *Proceedings of Symposia in Applied Mathematics*, Garrett Birkhoff and Eugene P. Wigner, Eds., vol. XI, p. 58, American Mathematical Society (1961).

7. F. Abbey (Comp.), *Handbook of Experimental Criticality Data, Part III*, British Report AHSB(S) Handbook 5, pp. 198–207 (1968).

8. J. K. Fox, L. W. Gilley, and E. R. Rohrer, *Critical Mass Studies, Part VIII, Aqueous Solutions of ^{233}U*, ORNL-2143 (September 1959).

9. A. Staub, D. R. Harris, and M. Goldsmith, "Analysis of a Set of Critical Homogeneous U-H_2O Spheres," *Nucl. Sci. Eng.* 34, 263–74 (1968).

10. F. Abbey (Comp.), *Handbook of Experimental Criticality Data, Part I*, British Report AHSB(S) Handbook 5, pp. 1–7 (1967).

11. J. K. Fox et al., *Neutron Phys. Div. Ann. Progr. Rep. Sept. 1, 1958*, ORNL-2609, p. 42.

12. S. R. Bierman and E. D. Clayton, *Status of HTGR Criticality Safety Data Needs on U-Th Fuel Cycle*, Research Report, (unnumbered) Battelle Pacific Northwest Laboratories (June 1975).

Appendix

ATOMIC COMPOSITION AND GEOMETRY OF CALCULATED CRITICAL SYSTEMS

Included in this appendix are tables which list the atomic composition and geometry of all the critical systems calculated in this work. Tables A1 and A2 describe the highly enriched ^{233}U critical experiments. Tables A3 and A4 characterize the two highly enriched ^{235}U critical experiments. Tables A5 and A6 give a description of three theoretical ^{233}U systems.

Table A1. Atomic number densities[a] of highly enriched ^{233}U critical experiments

Material	Experiment					
	1	2[b]	3	4	5	6
^{233}U	4.682(−2)	1.551(−3)	4.264(−4)	1.735(−4)	4.329(−5)	3.346(−5)
^{234}U	5.697(−4)	8.448(−6)	2.323(−6)	9.452(−7)	7.146(−7)	5.250(−7)
^{235}U	0	6.232(−7)	1.713(−7)	6.972(−8)	1.757(−8)	1.000(−8)
^{238}U	2.801(−4)	1.107(−5)	3.045(−6)	1.239(−6)	2.775(−7)	2.560(−7)
^{232}Th	0	0	0	0	1.964(−7)	1.476(−7)
N	0	0	0	0	1.182(−4)	7.530(−5)
H	0	6.111(−2)	6.567(−2)	6.611(−2)	6.641(−2)	6.647(−2)
O	0	3.370(−2)	3.370(−2)	3.341(−2)	3.365(−2)	3.353(−2)
F	0	3.141(−3)	8.639(−4)	3.515(−4)	0	0

[a](atoms/barn-cm).
[b]Reflector composition: H, 7.734(−2); C, 3.867(−2).

Table A2. Geometry description of highly enriched ^{233}U critical experiments

	Experiment					
	1	2	3	4	5	6
Geometry	Sphere	Cylinder	Cylinder	Sphere	Sphere	Sphere
Critical radius, cm	5.963	8.35	12.75	15.94	34.595	61.0108
Critical height, cm	--	16.7±0.2[a]	24.0	--	--	--
Reflector thickness, cm	None	20.0	None	None	None	None

[a]Extrapolated value derived from source neutron multiplication curve. Maximum subcritical height was 16.3 cm.

BLANK PAGE

Table A3. Atomic number densities[a] of highly enriched ^{235}U critical experiments

Material	Experiment 7	Experiment 8
^{234}U	4.915(−4)	5.864(−7)
^{235}U	4.511(−2)	4.774(−5)
^{238}U	2.411(−3)	2.864(−6)
H	0	6.650(−2)
O	0	3.335(−2)
F	0	1.024(−4)

[a](atoms/barn-cm).

Table A4. Geometry description of highly enriched ^{235}U critical experiments

	Experiment 7	Experiment 8
Geometry	Sphere	Sphere
Critical radius, cm	8.710	34.6
Reflector thickness, cm	None	None

Table A5. Atomic number densities[a] of three theoretical ^{233}U systems

Material	Case 1[b]	Case 2[b]	Case 3[b]
^{233}U	1.404(−2)	8.477(−4)	1.160(−4)
H	2.808(−2)	1.695(−3)	5.802(−2)
O	4.212(−2)	2.543(−3)	2.924(−2)
C	0	8.477(−2)	1.160(−2)

[a](atoms/barn-cm).
[b]Reflector composition: H, 6.666(−2); O, 3.333(−2).

Table A6. Geometry description of three theoretical ^{233}U systems

	Case 1	Case 2	Case 3
Geometry	Sphere	Sphere	Sphere
ENDF/B-III[a] calculated critical radius, cm	7.64	26.17	14.44
H-R[b] calculated critical radius, cm	8.25	29.5	15.1
Reflector thickness, cm	20.0	20.0	20.0

[a]Calculated values reported in Ref. 12.
[b]Calculated values reported in Ref. 3.